Tarek M. Madkour[*, ∂, €]
Bart Goderis[€]
Vincent B.F. Mathot[∀, €]
Harry Reynaers[€]

[€]**Katholieke Universiteit Leuven, Departement Scheikunde, Laboratorium voor Macromoleculaire Structuurchemie,**
Celestijnenlaan 200F, B-3001 Heverlee, Belgium

[∀]**DSM Research,**
P.O. Box 18, 6160 MD Geleen, The Netherlands

Mesoscopic and molecular modelling of the chain microstructure, conformation and crystallisation of polyolefins

Abstract

A review describing the latest advances in the mesoscopic and molecular modelling of polyolefins is presented. Mesoscopic investigation into the effects of sequence length and sequence length distribution on the reinforcement of stereoblock-stereoregular polyolefins has been performed. These polymers consist of alternating atactic sequences, which are amorphous and act as elastomeric chains, and isotactic sequences which, if long enough, will crystallise and act as physical reinforcing cross-links. According to simulated morphology, the degrees of crystallinity of the different samples have been predicted. Mechanical properties such as Young's modulus at small extensions are also predicted in terms of the block size of the alternating isotactic and atactic sequences. Molecular simulation investigation into the influence of the chain microstructure on the conformational behaviour of these polymers has been detailed. Characteristic ratios, calculated on the basis of the rotational isomeric state model, have indicated the increased extension of the polymer backbone with the increase in the side chain length. The lower characteristic ratio calculated for octene polymers may explain the experimental observation that polyoctene has a lower melting point than other polyolefins. Probability distribution surfaces constructed by the integration of the molecular dynamics trajectories indicated an increase in the probability of $g^{\pm}t$ joint states on the expense of $g^{\pm}g^{\pm}$ pairs with the increase in the side chain length.

Keywords: *review, esoscopic modelling, molecular modelling, chain conformation, morphology, crystallisation, polyolefins.*

1. Introduction

During the 1950s, polymer chemists succeeded in advancing polymer research several steps forward. Continued improvements in instruments for polymer study (such as the electron microscope and new forms of spectroscopy), detailed investigations into the behaviour of polymeric reactions, and accumulated industry know-how made possible the building of molecules by design. Control of properties at the molecular level led to an array of polymer uses and shapes. A major advance in polymer synthesis was the development of catalysts that exactly controlled the positioning of atoms attached to polymer chains, later known as stereoregularity. In 1953 a research team led by Karl Ziegler [1] discovered that organic compounds of metals, such as aluminium alkyl, enabled gas ethylene to polymerise at room temperature and at normal atmospheric pressure. Ziegler also found that his polyethylene did not consist of ethylene units randomly attached in a branched pattern, as was the case with the polymers produced by older methods. The compounds he and his co-workers had created contained very ordered, very long, straight-chain molecules. Shortly after Ziegler's group obtained their new polyethylene, Giulio Natta [2] announced that his laboratory in Milan had used a Ziegler catalyst to obtain a stereoregular polypropylene. In this polymer, the atoms of the propylene units that were not part of the main carbon chain occurred in a regular pattern either at one side or the opposing side of the chain. In his polymerisation of propylene, Natta obtained a mixture of a rubber-like substance and a plastic material. The only molecular difference between these two polypropylenes as outlined by Battjes & co-workers [3] was the position of the side groups on the chain. When units in the chain had the same side group placement, they were plastic. When the side groups were randomly placed, they created a rubber. Changing the catalyst altered the placement of these side groups. They were either isotactic (all on the same side of the chain), syndiotactic (alternately at one side and the opposing side of the chain), or atactic (randomly at one side or the opposing side of the chain). By using Ziegler-Natta catalysts, materials with special arrangement of side groups in naturally occurring polymers such as cis-polyisoprene, the natural rubber, could be duplicated as indicated by Warrick et al. [4] The manufacture of stereoregular polymers increases the degree of crystallinity, and with it the strength, modulus and density of the polymer. These catalysts are the basis of the production of high-density polyethylene (HDPE) and isotactic polypropylene. HDPE has improved thermal, mechanical, and chemical properties over low-density polyethylene [5]. Isotactic polypropylene, consisting of regular arrangements of stereocentres, is a crystalline thermoplastic material with a melting point of nearly 187.7°C, whereas atactic (stereorandom) polypropylene is an amorphous gum elastomer [5,6]. Natta [2], however, reported the polymerisation of rubbery polypropylene, which exhibits elastomeric properties attributed to a stereoblock microstructure. Blocks of crystallisable isotactic stereosequences and amorphous atactic sequences give rise to a

* To whom all correspondence should be addressed
∂ On leave of absence from the Department of Chemistry, Helwan University, Ain-Helwan, Cairo, Egypt 11795

thermoplastic elastomer. These elastomers, unlike vulcanised rubbers, soften and flow upon heating.

2. Metallocene catalyses

Many research groups [5,7-10] have reported a new strategy for the dynamic stereocontrol of the polymerisation of 1-olefins. They have described an olefin polymerisation catalyst, the metallocene catalyst, which was designed to isomerise between achiral (meso-like) and chiral (rac-like) coordination geometries in order to produce atactic-isotactic stereoblock polypropylene with interesting thermoplastic elastomeric properties. The behaviour of the catalyst has been interpreted in terms of its isomerisation, through rotations of the unbridged π ligands. Depending on the reaction conditions, a wide distribution of the isotactic and atactic sequences is obtained, which leads to polymer products with a wide variety of elastomeric properties. The microstructure of the polypropylene produced is considered to be built up of blocks of atactic and isotactic sequences, with the latter being of sufficient length to co-crystallise with similar sequences on the other polymeric chains. The rate of rotation of the catalyst ligands was shown using dynamic NMR to be quite rapid at room temperature; in fact, this process could not be frozen out even at -100°C [10]. A phenyl substituent on the indene ligand could in fact [5] inhibit the rate of ligand rotation such that it would be slower than that of monomer insertion yet faster than the time required to construct one polymer chain, so that it will produce long atactic and isotactic stereosequences. The high melting points (T_m ~ 137°C) of stereoblock polypropylene with low percentages of isotactic pentads (18% ≤ [mmmm] ≤ 73%) support a blocky structure for these materials [11,12]. Whole polymers produced using the metallocene catalysts consist of several fractions that could be separated using a series of boiling solvents. The properties of the various fractions vary from a semi-crystalline plastic (with a yield) for the highest isotactic content, otherwise referred to as the heptane-insoluble, to a weak gum elastomer with almost no isotactic content for the ether-soluble fraction. The hexane- or heptane-soluble fraction is elastomeric in nature, and thus indicates the presence of the stereoblock isotactic sequences along with the atactic sequences. The isotactic pentad content, [mmmm], increases with each successive fraction to reach ca. 70% for the hexane-insoluble fractions. The distribution of the block size also affects the mechanical properties of the stereoblock polypropylene. Natta [2] reported that, contrary to mixtures of amorphous and isotactic polymers with an overall crystallinity value up to 25% and accompanied by very low initial elastic modulus, stereoblock polypropylene with crystallinity values of 25% shows considerable elastic properties and reaches reversible elongation values up to 200%. Stress-strain diagrams [13] of stereoblock polypropylene indicate that such polymers have initial low elastic moduli, reversible elongation, and relative high tensile strength. The small creep values observed for these polymers could thus be attributed to the isotactic crystals acting as cross-links and thus opposing the flow of the chains [2,13]. The productivity of the catalyst as well as the molecular weight of the produced polymers was found to be sensitive to the reaction conditions [5,14]. The increase in the propylene pressure and the decrease in the polymerisation temperature usually lead to an increase in the molecular weight, probably because of the increase in the monomer concentration and the slowing down of the ligand rotations. High molecular weights could also be obtained using metallocenes [10], a possible consequence of high regioselectivity [15]. However, molecular weight of the produced polypropylene had lower values than those produced using industrial catalysts [16]. This is probably due to the increased rate of chain termination and / or the decreased rate of olefin insertion [17]. While polyolefins obtained with heterogeneous catalysts have large polydispersities of M_w / M_n = 5~10 [18], homogeneous catalysts produce polymers with polydispersities of 1.5~2.8 [19]. This was also predicted using the Schultz-Flory statistics [20] for polymers arising from identical catalyst centres with fixed rates of chain propagation and chain termination. Equilibrium melting points were shown [16] to increase with the increase in molecular weight and the decrease in (narrowing of) the molecular weight distribution.

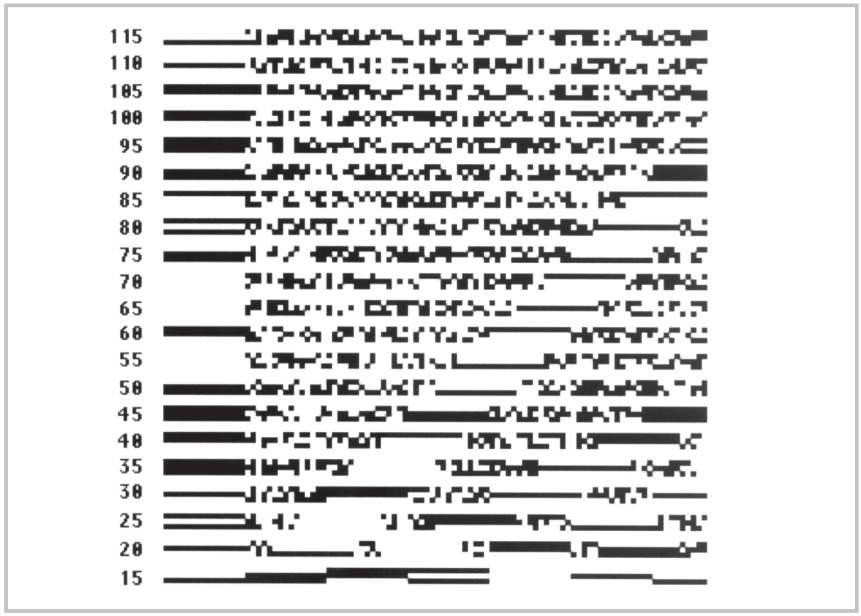

Figure 1. *Graphic representation of simulated chains of stereoblock polypropylene of various section repeat lengths. The black and white squares represent the (d) and (l) stereoisomers respectively.*

The metallocene catalysts are usually activated by the presence of MAO, methylaluminoxane cocatalyst. Ewen [21] indicated that a C_2-symmetric ethanobridged-indenyl-titanocene / MAO system is catalytic enough to perform effective homogeneous isospecific propylene polymerisation. Titanocene diphenyl, on the other hand, was shown to afford isotactic polypropylene with a different microstructure. The microstructure of the polymer produced using the former catalyst indicated an enantiomorphic-site control, while that of the latter indicated a chain-end control [21,22]. Polymerisation activities, stereoregularities, and polymer molecular weight were all shown to depend strongly on the co-catalyst identities and concentrations, thus suggesting strong structure-sensitive ion-pairing effects. Accordingly, it seems that the unbridged metallocene catalyst follows a two-state propagation mechanism [23]. The two different schemes eventually determine the configuration of the adding monomer units to the growing chains. These are the chain-

end control and the enantiomorphic-site control, otherwise known as the catalyst control [24].

In the former, the catalyst may provide necessary steric hindrance, but the configuration of the chain ends determines the configuration of adding monomer units according to a Bernoullian probability [25]. In the latter, the catalyst is considered to consist at any given time of an equal number of D and L preferring sites. D or L preferring sites will influence the configuration of the adding units to be either (d) or (l) respectively as defined in the older terminology, without the influence of the configurations of the chain ends [26]. Polymers produced using these two different schemes would have different microstructures. The first scheme would tend to give polymer chains of the type ddddllll; a defect in this case is followed by units of a similar configuration. Alternatively, the other scheme will produce a polymer of the type ddddldddd, known thus as the self-correcting propagation scheme. The probability that an adding unit in the second case would have the same configuration as the preference of the catalyst (D or L) at that particular site is known as the enantiomorphic probability, α [24]. Accordingly, P_{dd}, in the first case will equal P_{ll}, which is the probability that a chain end will add a unit of the same configuration, also known as the replication probability, P_r. In the second case, $P_{ld} = P_{dd} \neq P_{ll} = P_{dl}$ implying that [24], at D preferring sites, P_{dd} is greater than P_{dl}, whereas P_{dd} at the D preferring sites will equal P_{ll} at the L preferring sites, so that α would usually have a value of 0.5 or higher.

3. Nmr microstructure analysis

The nine resolvable pentad signals of polypropylene as observed by NMR experiments could be used to differentiate between the two propagating schemes used to produce polypropylene stereochemical structures. Stereoblock polymers produced from catalysts with chain-end control (Bernoullian mechanism) have the predominant stereochemical defect as mmrm, and the population ratios of the major pentads are [14]:

mmmr : mmrr : mrrm: mmrm = 1 : 0 : 0 : 1

where m refers to a pair of polypropylene units with similar configurations (meso), and r refers to a pair of polypropylene units with opposite configurations (racemic). The self-correcting propagation is observed by the signal mrrm. The population ratio of the isolated racemic pentads in this case will be in the order of [14]:

mmmr : mmrr : mrrm: mmrm = 2 : 2 : 1 : 0

The sensitivity of the polymer microstructure to the reaction conditions [27] could be depicted by evaluating the isotactic pentad content, [mmmm].

Increasing propylene pressure and decreasing polymerisation temperatures always increase the isotactic pentad content, which is probably due to the effect of monomer concentration on the rate of monomer enchantment at both sites of the catalyst, the rate of catalyst isomerisation being independent of the monomer concentration. Lowering the polymerisation temperature would, however, slow down the rate of the catalyst isomerisation, and allows for longer sequence propagation times [28].

Statistical modelling of the ^{13}C NMR spectra of the polypropylene produced using these catalysts could not be accommodated with simple Bernoullian, first-, second-order Markovian or enantiomorphic-site control propagation statistics [28,29], which implies that the polymerisation mechanism follows the two-state propagation scheme [23]. Cheng [30,31] has formulated perturbed probability analytical equations based on the perturbations of the Bernoullian or the Markovian reaction probabilities that take into account the chain-end control and the enantiomorphic-site control schemes.

4. Influence of reaction conditions

As discussed earlier, due to the isomerisation of the metallocene catalysts between the achiral and chiral coordination geometries, atactic-isotactic stereoblock polypropylene is produced. Depending on the reaction conditions, a wide distribution of the isotactic and atactic stereosequences is obtained (see Figure 1), which leads to polymer products with a variety of elastomeric properties [10]. This, however, could be evaluated by investigating the isotactic pentad content, [mmmm]. Increasing propylene pressure and decreasing polymerisation temperature always increases the isotactic pentad content. This might [23] be due to the effect of monomer concentration, [mon], on the rate of monomer enchantment at either site of the catalyst with

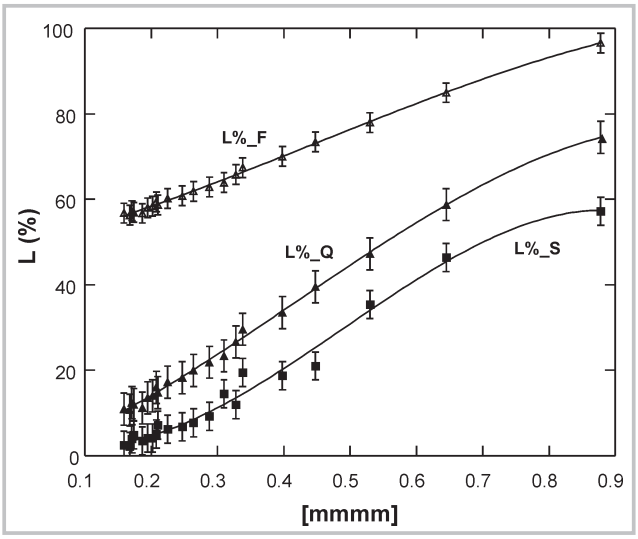

Figure 2. Degree of crystallinity of the polymers as a function of the isotactic pentad content, [mmmm].

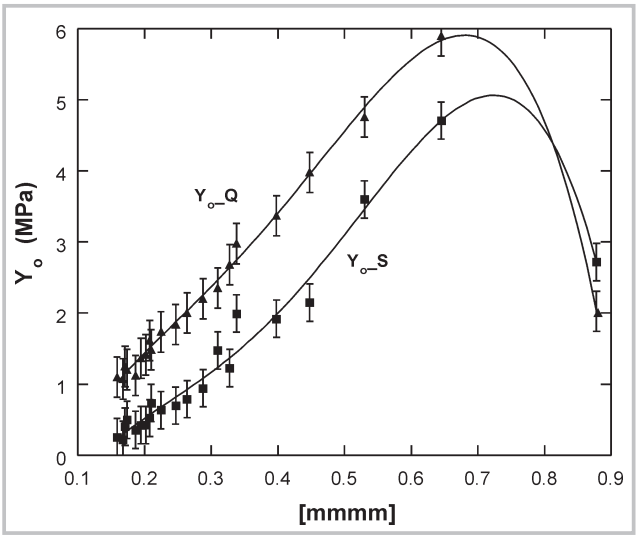

Figure 3. Young's modulus at infinitesimal extension as a function of the isotactic pentad content, [mmmm].

the rate of the isomerisation of the catalyst independent of [mon]. Propene polymers obtained at room temperature had rather low degrees of polymerisation [32]. This must be due to an increased rate of chain termination and / or to a decreased rate of olefin insertion. Nevertheless, the higher the temperature, the faster the rotations of the ligands, and consequently shorter block sequences can be expected to be produced. This corresponds experimentally to the lower isotactic pentad content observed at higher temperatures. By varying the catalyst structure and polymerisation conditions, it might be possible to produce elastomeric polypropylene that exhibits reinforced elastic properties [14]. Bridged metallocene catalysts produce elastomeric polypropylene that is uniform in composition, completely soluble in ether and features a narrow molecular weight distribution. Zirconium catalysts, unlike the titanium ones, produce low molecular weight material. The catalyst is less active and in general unstable at conventional polymerisation temperatures [33].

Titanium metallocenes failed to provide significant quantities of polypropylene in toluene solution between -50 °C and -80°C. The small amount produced was predominantly isotactic in nature. The productivity was substantially higher at conventional temperatures [14]. The zirconium and hafnium metallocenes, however, exhibited higher productivity. Interestingly enough, hafnium catalysts are significantly more stereoregulating than their zirconium counterparts. This is probably due to the rate of interconversion between the two states during polymerisation. Changing the bridging atom from carbon to silicon had a significant effect on the molecular weight of the polymer produced using these bridged metallocene catalysts [14]. This was due to the decrease in the rate of chain transfer processes. Consequently, elastomeric properties of polypropylene were shown to depend to a great extent on the type of catalyst being used. Catalysts that are capable of producing higher molecular weight and more stereoregular polymers were found to give rise to materials with high ultimate extensions and excellent elastic recoveries with toughness.

5. Kinetics of polymerisation

The kinetics of polymerisation, based on the Coleman-Fox multistate mechanism theory [23], takes into account both the chain-end and the enantiomorphic-site control propagation schemes.

When the metallocene catalyst is in the cis-position, atactic sequences are produced using a chain-end control propagation mechanism. On rotation, the catalyst switches to the trans-isomer, thus producing isotactic sequences using an enantiomorphic-site control propagation scheme. Polymerisation is carried out according to [34]: *

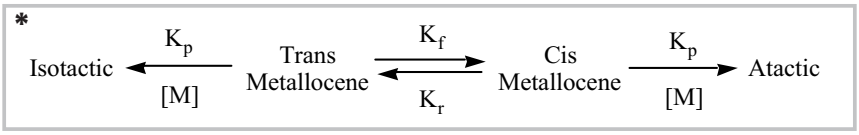

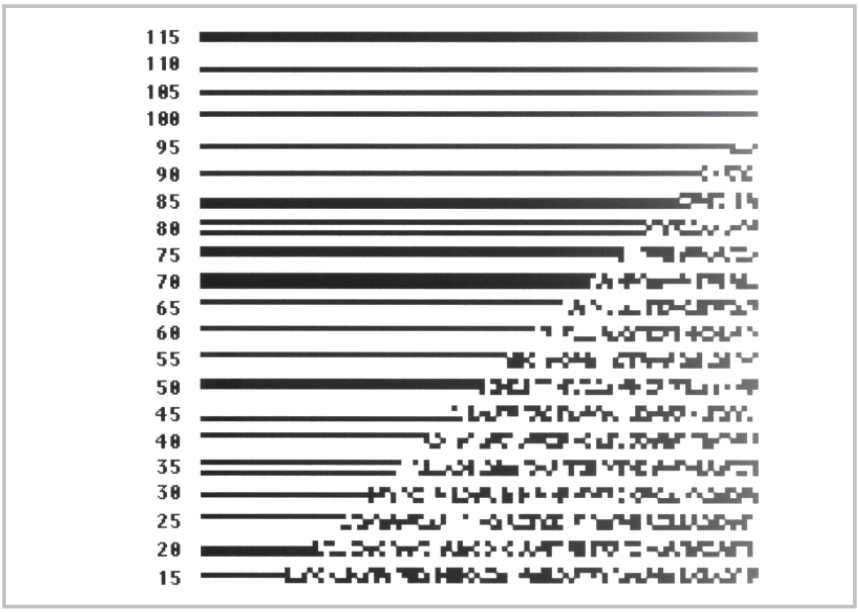

Figure 4. *Degree of crystallinity of the polymers as a function of the isotactic pentad content, [mmmm].*

The rate of rotation of the metallocene catalyst is characterised by the rate constants K_f and K_r of switching from the trans- to the cis-positions and vice versa respectively. Consequently, the reactive end of a growing chain would exist in two possible states that are in dynamic equilibrium:

$$K_f\,[\text{trans}] = K_r\,[\text{cis}] \qquad (1)$$

The rate constant of this rotation, otherwise referred to as the equilibrium rate constant K_{eq}, is defined by:

$$K_{eq} = K_f \,/\, K_r = [\text{cis}] \,/\, [\text{trans}] \qquad (2)$$

At a K_{eq} of 1, there must be as many cis-isomers of the catalyst as there are trans isomers. Each one of these states is thus capable of adding a monomer unit with its own rate of propagation, R_p. In both cases, however, the monomer units add to the growing chain with a rate constant K_p, since the rate of the catalyst rotation is slow enough to allow for the insertion of many consecutive monomeric units to a single sequence. The propagation rate constants of the cis- and trans-isomers as compared to that of the ligand rotation could be safely assumed to equal each other, known as the special case II of the Coleman-Fox theory [35]. The rate of propagation of isotactic and atactic sequences could thus be calculated from:

$$R_p\,(\text{isotactic}) = K_p\,[M][\text{trans}] \qquad (3a)$$

$$R_p\,(\text{atactic}) = K_p\,[M][\text{cis}] \qquad (3b)$$

However, the rate of initiation (formation), R_I, of the cis- and trans-metallocene catalysts must be related to the amount of cis- and trans-isomers available during the polymerisation reactions. These are given respectively by:

$$R_I\,(\text{trans}) = K_r\,[\text{cis}] \qquad (4a)$$
$$R_I\,(\text{cis}) = K_P\,[\text{trans}] \qquad (4b)$$

The kinetic chain length (υ) of a particular sequence is defined by [36]:

$$\upsilon = \frac{\textit{rate of addition of molecules to growing chains}}{\textit{rate of formation of growing chains}} = \frac{\textit{rate of propagation}}{\textit{rate of initiation}} \qquad (5)$$

Therefore, the average block length of the isotactic and the atactic sequences, υ_i and υ_a, respectively, could be calculated from:

$$\upsilon_i = K_p\,[M][\text{trans}] \,/\, K_r\,[\text{cis}] \qquad (6a)$$

$$\upsilon_a = K_p[M][cis] / K_f[trans] \quad (6b)$$

At dynamic equilibrium, $K_f[trans] = K_r[cis]$. Therefore,

$$\upsilon_i = K_p[M][trans] / K_f[trans] = K_p[M] / K_f \quad (7a)$$

and,

$$\upsilon_a = K_p[M][cis] / K_r[cis] = K_p[M]/K_r \quad (7b)$$

The relationship between both average lengths could thus be calculated from:

$$\upsilon_i/\upsilon_a = (K_p[M]/K_f) \times (K_p[M]/K_r) = K_r/K_f = 1/K_{eq} \quad (8)$$

or,

$$K_{eq} = \upsilon_a/\upsilon_i \quad (9)$$

which implies that the average block length of atactic sequences is related directly to that of the isotactic sequences by the rate of the catalyst rotation which naturally depends on the reaction conditions. Given the average block length of isotactic sequences, υ_i, the rate constant of the ligand rotation, K_{eq}, the Bernoullian (replication) probability, P_r, and the enantiomorphic probability, α, fully representative polymeric chains could thus be simulated.

6. The polymerisation model

The model of polymerisation assumes the randomness of the stereochemistry of the first sequence, isotactic or atactic. If isotactic, a preference is thus randomly given to the catalyst site, which is further used along with the enantiomorphic probability, α, to simulate this particular sequence. The lengths of all the isotactic sequences are determined by the average block length of isotactic sequences, υ_i, on a Gaussian distribution. If, however, the sequence was determined to be atactic, its length could be calculated using υ_i and K_{eq} on a Gaussian distribution. The configuration of the first unit of this atactic sequence is determined randomly, and that of every consecutive unit is determined by comparing the replication probability, P_r, to a random number [37]. Other isotactic and atactic sequences are simultaneously simulated according to the above-described propagation schemes to assemble the polymeric chains fully with respect to their microstructures (see Figure 1).

The major nine pentads, mmmm, mmmr, rmmr, mmrr, mmrm, rmrr, mrmr, rrrr, mrrr, and mrrm, are calculated by examining the stereochemical structure of the simulated polymeric chains for every different set of the polymerisation parameters υ_i, K_{eq}, P_r, and α, and are further compared to those determined experimentally using NMR techniques [26]. The effect of these parameters on the pentad signals is made obvious by examining the change in the major pentads, mmmm, mmrm, and mrrm. As mentioned earlier, the last two pentads are synonymous with the chain-end control and the enantiomorphic-site control propagation schemes respectively. The investigation should therefore provide enough information on the effect of the reaction conditions on the propagation schemes. The relationship between the polymerisation parameters and the reaction conditions could be inferred from observing the change in the mmmm signal as the increase in the propylene pressure and the decrease in the polymerisation temperature, T_p, always increases mmmm distribution values. Sliding the chains past one another longitudinally to search for the largest possible number of matches was carried out on model annealed samples (searched, „S" as opposed to quenched, „Q"). The longitudinal movement of the chains relative to one another, out of register, approximately models the lateral sorting out of sequences in polymeric chains during the annealing process. In sliding the chains by one another in these searches, protruding sections were relocated from one end of the array to the other so as to keep the number of comparison pairs constant.

7. The degree of crystallisation

Each unit in the chains was given the opportunity to be involved in the crystallisation process so long as they occurred in a sequence of a minimum length suitable for crystallisation and neighboured with other isotactic sequences on neighbouring chains. The minimum number of units in a sequence required for crystallisation is taken to be fourteen units [6]. This number corresponds to the thickness of the smallest crystallite (3.0 nm) detected for the ether-soluble elastomeric low range isotactic polypropylene. Isotactic sequences in proper arrangements [38] with neighbouring sequences and of sufficient sequence length would be expected to crystallise

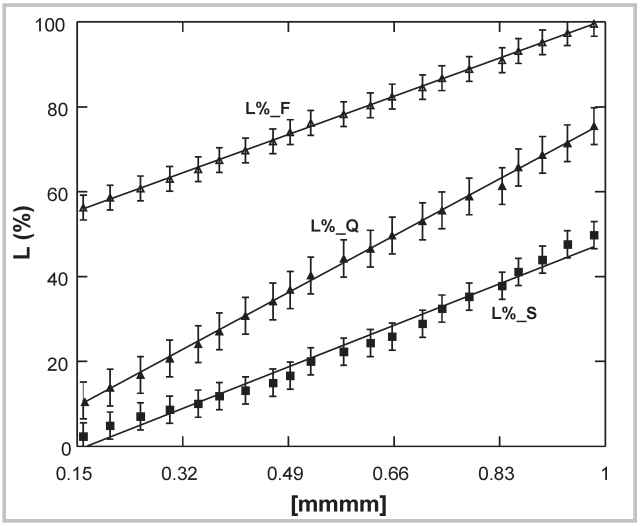

Figure 5. Degree of crystallinity of the polymers as a function of the isotactic pentad content, [mmmm].

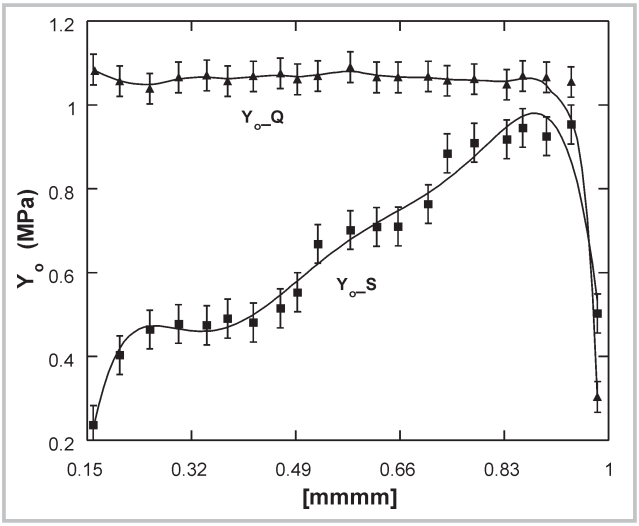

Figure 6. Young's modulus at infinitesimal extension as a function of the isotactic pentad content, [mmmm].

[39-42]. Crystallites formed during slow crystallisation would grow longitudinally until meeting a unit of the other type, and laterally so long as sequences of the crystallisable component of a minimum sequence length were available from the amorphous regions. Values of the degree of crystallinity of the various samples simulated were determined by counting the units involved in the melting sequences relative to the total number of units. The results are shown in Figure 2 as a function of [mmmm]. As expected, the degree of crystallinity increases with [mmmm] as a consequence of the increase in the crystallisable isotactic content.

The chain-matching process only resulted in the decrease of the percent crystallinity values. The crystallinity values predicted for the quenched and searched (annealed) cases are obviously less than those predicted using the melting point depression relationship [20], and are more comparable to values determined experimentally [14]. It should be noted here that for the whole range of [mmmm] crystallinity had a positive value, in contrary to atactic polypropylene which shows no sign of crystallinity. This crystallinity is the result of the presence of the isotactic blocks in the stereoblock polypropylene, which are capable of segregation and separation from the amorphous part of the polymer to form crystallites. These crystallites would act as cross-links, thus reinforcing the polymer networks and causing the attractive properties of stereoblock polypropylene as illustrated by Natta [2].

8. Moduli of the elastomeric networks

The theory of rubber-like elasticity theory [43,44] relates the modulus of elasticity to the number of crystalline sequences acting as cross-links, with the sequences in the amorphous state contributing as elastomeric chains. If the number of crystalline sequences per unit volume is represented by υ_c, then Young's modulus at infinitesimal deformations is given by

$$Y_o = 3RT\,(\upsilon_c / N_1) \qquad (10)$$

where
N_1 is the number of the units actually participating in the formation of the crystallites. The values of Young's modulus predicted from the simulated

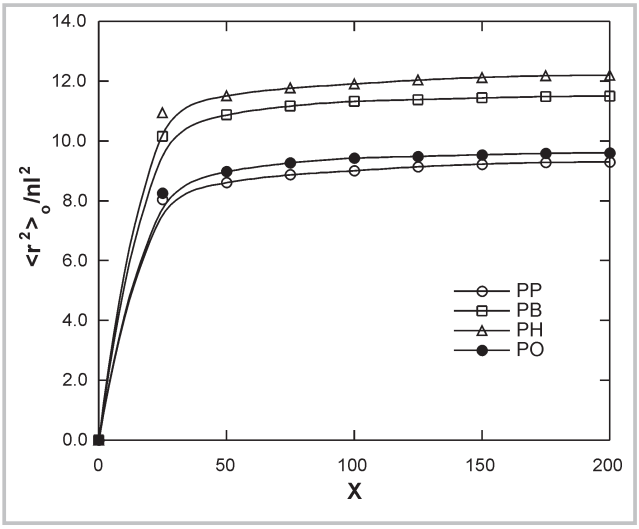

Figure 7. Characteristic ratio, $C_n=\langle r^2\rangle_o/nl^2$, of isotactic PP, PB, PH, and PO as a function of the degree of polymerisation, X, calculated at 473K.

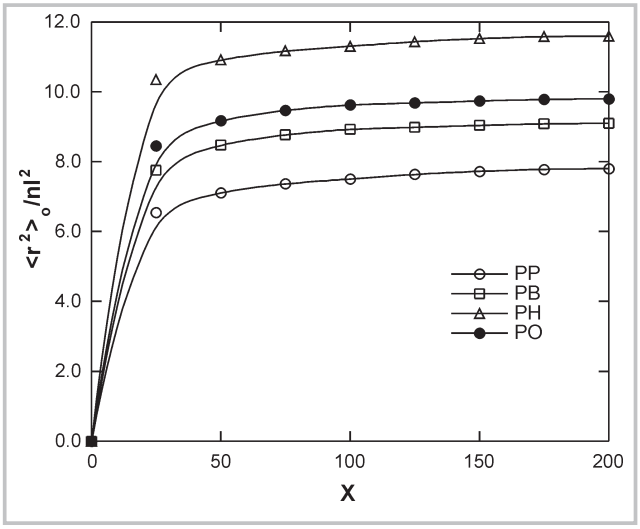

Figure 8. Characteristic ratio, $C_n=\langle r^2\rangle_o/nl^2$, of syndiotactic PP, PB, PH, and PO as a function of the degree of polymerisation, X, calculated at 473K.

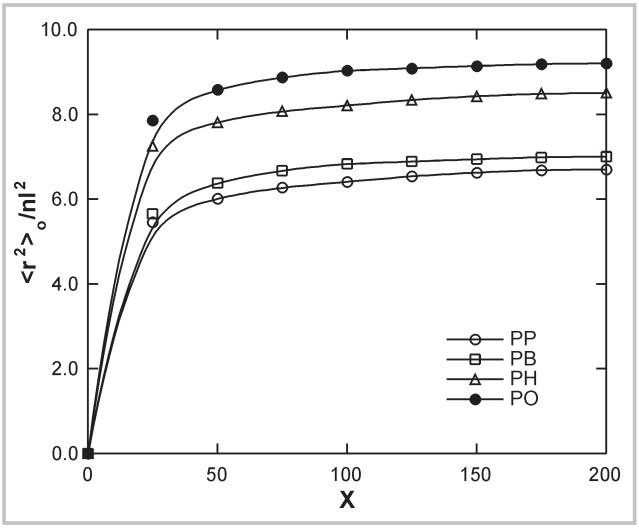

Figure 9. Characteristic ratio, $C_n=\langle r^2\rangle_o/nl^2$, of atactic PP, PB, PH, and PO as a function of the degree of polymerisation, X, calculated at 473K

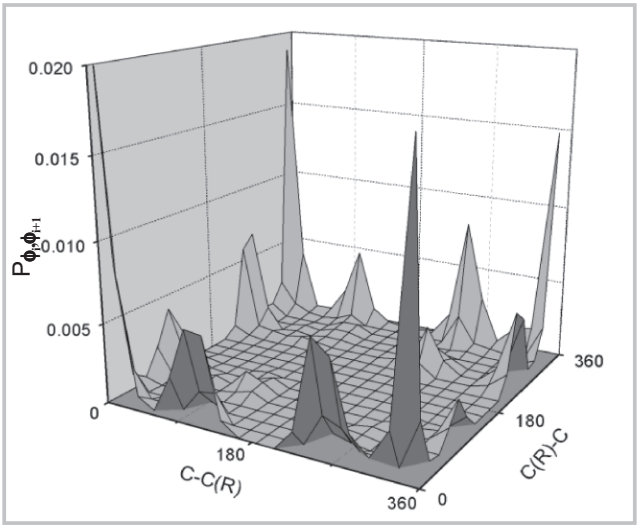

Figure 10. Probability distribution surface $P(\phi_i,\phi_{i+1})$ for the torsional angles (ϕ_i,ϕ_{i+1}) of polyethylene

values of υ_c are shown in Figure 3. As indicated in the figure, a wide variety of polypropylene samples with different mechanical properties could thus be produced depending on the isotactic content of these samples. The samples could range from plastic polymers with higher initial elastic modulus, higher tensile strength and lower elastic elongation, to true elastomeric polypropylene.

9. Effect of block size

Different stereoblock polypropylene fractions of increasing isotactic block lengths were also simulated using Monte Carlo methods to model the effect of increasing the isotactic block length. Every simulated chain is divided into equally long sections, and every section will consist of one isotactic sequence as well as one atactic sequence. For all the computations carried out in this case, the increase in the length of the isotactic sequences is made at the expense of the length of the atactic ones in order to keep the section length constant. An illustration of this arrangement is shown in Figure 4.

The increase in the isotactic block length will naturally be reflected on the values of the isotactic pentad content, [mmmm]. The values of the degree of crystallinity of various polypropylene samples with different isotactic block sizes are shown in Figure 5 as a function of [mmmm]. As expected, the degree of crystallinity increases with [mmmm] as a consequence of the increase in the crystallisable isotactic content. The chain-matching process also resulted in the decrease of the percentage crystallinity values. The values of Young's modulus predicted from the simulated values of υ_c in this case are shown in Figure 6. It is obvious from the figure that the increase in the isotactic block length might have had an increasing effect on the thermodynamic properties of crystallisation, but had no effect on Young's moduli for almost all the range of the isotactic content. This is because the elasticity of the samples will only depend on the number of the amorphous sequences present within the polymeric networks. At the vicinity of high isotactic content, the number of the amorphous sequences decreases as a result of the joining of the crystalline isotactic sequences, hence the drop of the elastomeric moduli.

10. Chain conformational analysis

Conformational analysis of polyolefins could be achieved using the rotational isomeric state model (RIS) [45-47]. RIS is normally used for vinyl chains for the calculation of the random-coil unperturbed dimensions $\langle r^2 \rangle_o$ of polyolefins such as polyethylene chains [45,48] and polypropylene chains of various stereochemical compositions [48]. The characteristic ratio is thus given by:

$$C_n = \left\langle r^2 \right\rangle_0 / n l^2 \qquad (11)$$

The characteristic ratios C_n calculated according to Eq 14 for the various 1-olefin homopolymers are shown in Figures 7, 8 and 9 for the isotactic, syndiotactic, and atactic homopolymers, respectively.

A gradual increase in C_n was observed for all the different homopolymers with X, the degree of polymerisation (which levels off around X=100) indicating that the characteristic ratio at these levels is very close to its value in the limit of very large X. This is also an indication that the value of 200 units chosen for the degree of polymerisation for the homopolymers and the copolymers is sufficiently high, and that the behaviour of the characteristic ratio at this value is independent of the degree of polymerisation and rather dependent on the nature of the chain microstructure of the various polymers. For the isotactic case, Figure 7 illustrates the natural increase in C_n with the increase in the side chain length, since chains with a larger substituent are highly strained and experience stronger repulsive first-order interactions. The behaviour observed is consistent with suggestions that persistence length begins to increase owing to an increase in the side group length [49]. Interestingly, a further increase in the side chain length results in the eventual decrease in the characteristic ratio, as is the case with 1-octene homopolymer. This abnormal result is due to the increased frequency for potential overlaps between the long side chains, giving rise to third- and higher-order interactions. These side chains mutually exclude each other from otherwise accessible space, and the longer the side chain is, the more relevant this space exclusion must be. At such a point, when the side chains are long enough and much more excluded space is therefore necessary, the main backbone chain may have to coil onto itself to allow the longer side chains to point outwards, giving rise to a much lower value of the unperturbed end-to-end distance and subsequently lower values for the characteristic ratio.

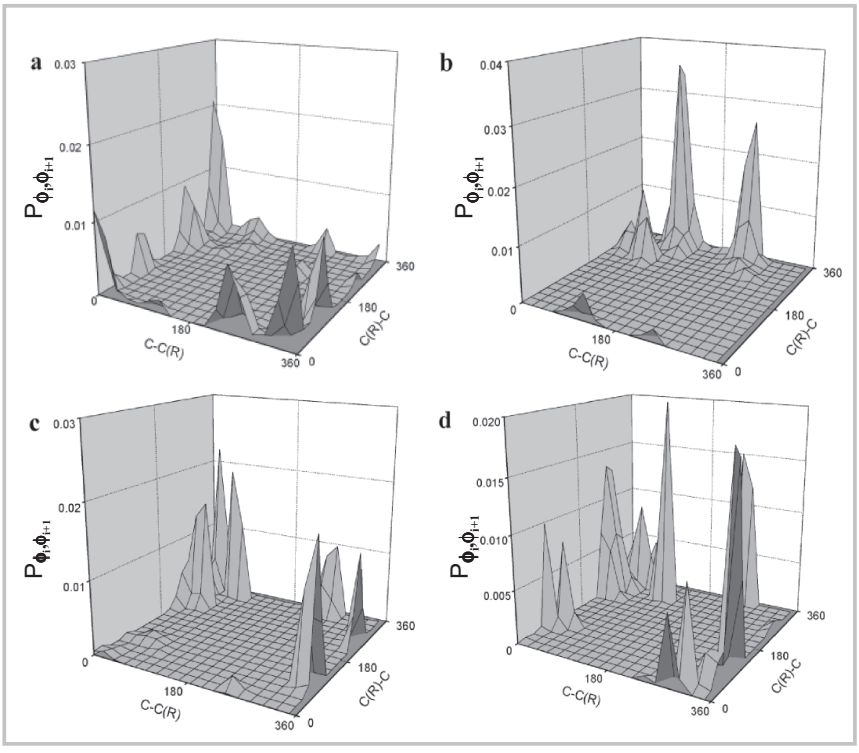

Figure 11. *Probability distribution surfaces $P(\phi_i,\phi_{i+1})$ for the torsional angles (ϕ_i,ϕ_{i+1}) in case of isotactic homopolymers.*

This conformational behaviour may in fact explain the experimental observation that some sort of transition in the physical properties such as the specific volume or the intrinsic viscosity of poly(1-olefin)s does occur with the inflection point around the poly(1-hexene) and / or poly(1-heptene) [51,52], with the melting point observed for poly(1-octene) as low as –20 °C. Similar observations could also be obtained for the syndiotactic cases (Figure 8). The curtailed increase in the characteristic ratio of the syndiotactic polymeric chains with the increase in the side chain length is due to the influence of the syndiotactic placements in obstructing the perpetuation of the preferred helix conformation for the perfect isotactic chain. The physical basis for these results is that the syndiotactic chain is being forced toward the helical conformation represented by $(g^+g^+)(tt)(g^-g^-)$ $(tt)(g^+g^+)(tt)$, etc. Comparison between the results obtained for stereoregular cases (Figures 7 and 8), and those obtained for the irregular atactic polymer chains (Figure 9), indicates the sensitivity of the unperturbed dimensions of the polymeric chains to the stereochemical microstructure.

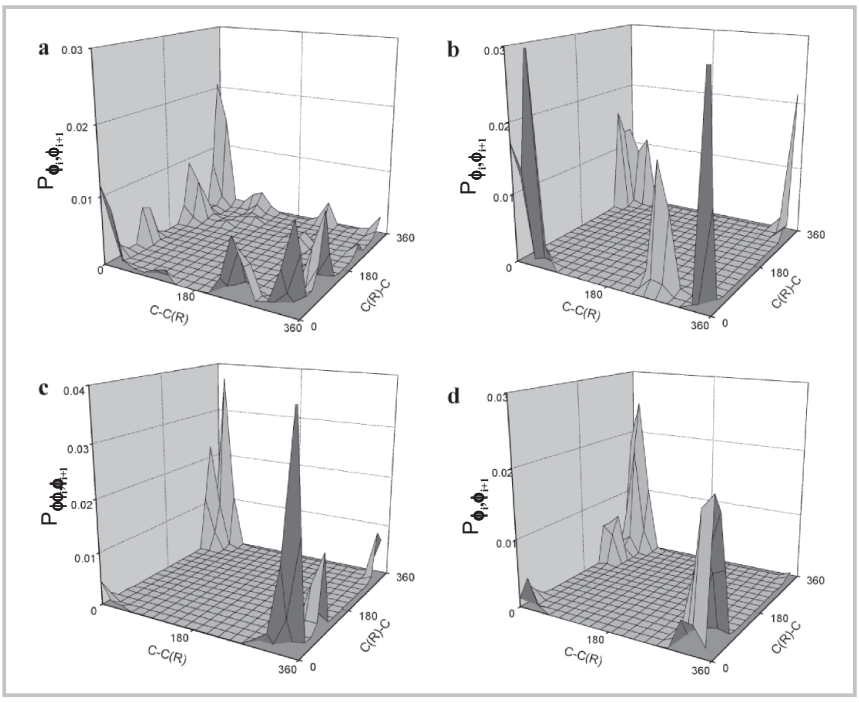

Figure 12. *Probability distribution surfaces $P(\phi_i,\phi_{i+1})$ for the torsional angles (ϕ_i,ϕ_{i+1}) in the case of syndiotactic homopolymers.*

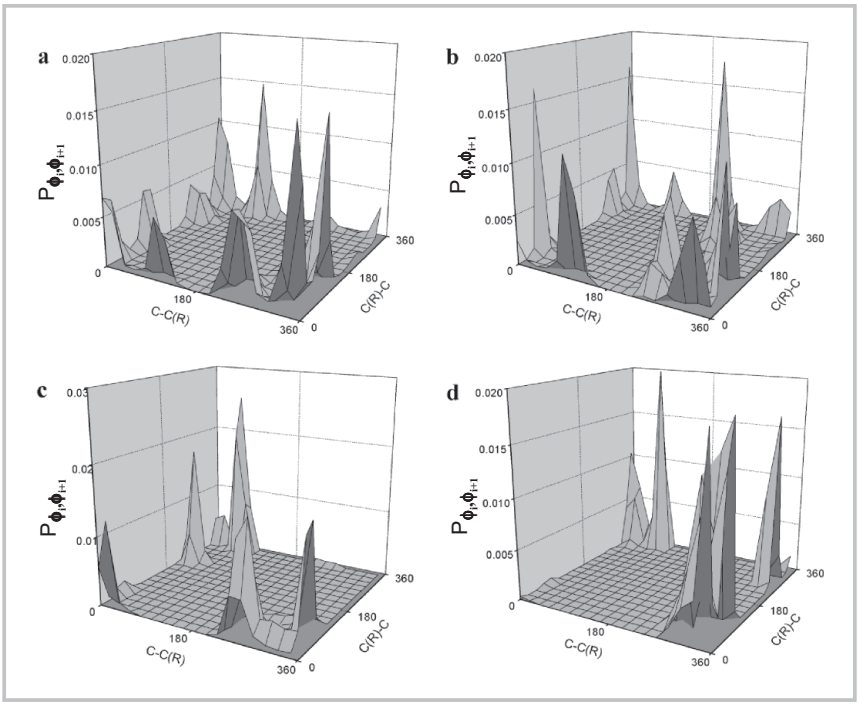

Figure 13. *Probability distribution surfaces $P(\phi_i,\phi_{i+1})$ for the torsional angles (ϕ_i,ϕ_{i+1}) in the case of atactic homopolymers.*

In the case of the atactic polymer, C_n did increase with the increase in the side chain length, but showed no maximum at PB or PH. In fact, PO had the highest C_n of all studied atactic homopolymers due to the lessening of the side group crowding effect.

11. Probability distribution surfaces

Following the method of Mattice et al. [52], utilising molecular dynamics simulations of polymeric fragments of ten repeat units in vacuum at 473K using the Cerius^2 software package (MSI) and employing the COMPASS forcefield [53], the probability distribution surfaces of poly(1-olefins) could be evaluated. The duration of the simulations was chosen to be long enough (10 ns) to allow sufficient sampling of the conformational space. In all cases, the initial conformation, where all the internal backbone bonds are in the trans state, was minimised using a conjugate gradient method. The simulation was then performed by using the Verlet algorithm [54] to integrate the equation of motion for all atoms with time increments of 0.5 fs. Hydrogen atoms were included explicitly.

Isothermal conditions were maintained by rescaling the instantaneous velocities of the atoms at intervals of 1 ps. From the history of dihedral angles, a wide variety of torsional states was observed to have been visited by the backbone bonds of all the fragments, with substantial fluctuations taking place over time ranges of picoseconds. However, a closer examination of the time and space distribution of dihedral angles indicated that the torsional motions of the two bonds centred about the carbon atoms bearing the side chains are not independent of each other but occur in a concerted fashion. A systematic analysis of pair correlation between neighbouring bonds is made possible by examination of the probability distribution surfaces constructed as a function of two consecutive bond rotations (Figures 10-13). The basic procedure involves the

consideration of the conformational space defined by the complete revolutions of two adjacent bond angles, ϕ_i and ϕ_{i+1}, dividing it into small subspaces (36 x 36) of dimensions ($\Delta\phi_i$, $\Delta\phi_{i+1}$) = (10^o, 10^o) and recording the overall residence time in each subspace. Normalisation of the latter yields the probability $P(\phi_i,\phi_{i+1})$ of occurrence of the joint state (ϕ_i,ϕ_{i+1}) representative of a given subspace. Figure 10 illustrates the probability distribution surface for polyethylene. In the figure, it is obvious that the most preferred dihedral angle pair correlation is tt which has the highest probability of occurrence. The dihedral pairs of $tg^{\pm}$ and $g^{\pm}t$ do exist but with less probability of occurrence, followed by a small probability for the pairs $g^{\pm}g^{\pm}$, in complete agreement with the well-known data for polyethylene [45,48]. Figures 11, 12 and 13 represent the probability distribution surfaces for the various isotactic, syndiotactic and atactic homopolymers respectively. In all the figures, a refers to PP, b refers to PB, c refers to PH and d refers to PO. Figure 11 indicates the influence of increasing the side chain length in case of the isotactic homopolymers on the probability of occurrence of a joint state. It is obvious that the increased length of the side chain has increased the probability of the joint states $g^{\pm}t$ on the expense of $g^{\pm}g^{\pm}$ pairs leading, therefore, to an apparent extension of the polymeric chains. A further increase in the side chain length, as is the case of PO, has actually reversed this effect as evident by its probability distribution surface. This could be illustrated by considering the proximity of the side chains in a polymer with large substituents.

The side chains are separated by only two bonds in the main chain between the sites of attachments of the branches; the first atoms in the two successive branches can participate in a second-order interaction. Side chain crowding near the backbone produced by a possible high density of the side chains will occur.

This will lead to short range interactions of higher order contribution to the overall configuration partition function. Similar behaviour was also obtained for the syndiotactic stereochemical structures (Figure 12). Interestingly, syndiotactic PO had a better-ordered pair correlation than isotactic PO, which is due to the lessening in the side chain crowding resulting from the configurational placements of the side chains along the two sides of the polymer backbone.

The large substituents, all placed on the same side of the backbone as in the case of isotactic PO, force the main backbone to favour more the gauche$^+$ and gauche$^-$ dihedral states in order to accommodate the side chain crowding. In the case of syndiotactic PO, the side chains force the polymer chain to assume more of the trans-torsional angle in order to accommodate the large size of the substituents placed opposite each other along the main backbone. The atactic polymers (Figure 13), as would be expected, show less order for the pair correlation of the dihedral angles as compared to both the isotactic and syndiotactic polymers (Figures 11 and 12).

❑

References

1. K. Ziegler, E. Holzcamp, H. Breil, H. Martin, Angew. Chem., 67, 541, (1955).
2. G. Natta, J. Polym. Sci., 34, 531, (1959).
3. K. Battjes, C. Kuo, R. Miller, J. Saam, Macromolecules, 28, 790, (1995).
4. E. Warrick, O. Pierce, K. Polmanteer, J. Saam, Rubber Chem. Technol, 52, 437, (1979).
5. G. W. Coates, R. M. Waymouth, Science, 267, 217, (1995).
6. T. M. Madkour, J. E. Mark, J. Polym. Sci., Polym. Phys. Ed., 35, 2757, (1997).
7. J. W. Collette, C. W. Tullock, R. N. MacDonald, W. H. Buck, A. C. L. Su, J. R. Harrell, R. Mülhaupt, B. C. Anderson, Macromolecules, 22, 3851, (1989).
8. D. T. Mallin, M. D. Rausch, Y. G. Lin, S. Doug, J. C. W. Chien, J. Am. Chem. Soc., 112, 2030, (1990).
9. L. Cavallo, P. Corradini, G. Guerra, Polym. Mat. Eng. Sci, 74, 421, (1996).
10. G. W. Coates, M. D. Bruce, R. M. Waymouth, Polym. Prepr, 37, 337, (1996).
11. S. Newman, J. Polym. Sci., 47, 111, (1960).
12. S. Z. Cheng, J. J. Jonimak, A. Zhang, E. T. Hsieh, Polymer, 32, 648, (1991).
13. G. Natta, G. Mazzanti, G. Grespi, G. Moraglio, Chim. e ind., 39, 275, (1957).
14. W. J. Gauthier, J. F. Corrigan, N. J. Taylor, S. Collins, Macromolecules, 28, 3771, (1995).
15. A. Grassi, A. Zambelli, L. Resconi, E. Albizzati, R. Mazzocchi, Macromolecules, 21, 617, (1988).
16. L. Resconi, R. Jones, A. Rheingold, G. Yap, Organometallics, 15, 998, (1996).
17. H. Brintzinger, D. Fischer, R. Mülhaupt, B. Rieger, R. Waymouth, Angew. Chem. Int. Ed. Engl., 34, 1143, (1995).
18. N. Kashiwa, Polymer, 12, 603, (1980).
19. W. Kaminsky, M. Miri, H. Sinn, R. Woldt, Makromol. Chem. Rapid Commun., 4, 417, (1983).
20. P. J. Flory, Principles of Polymer Chemistry, Cornell University Press, Ithaca, New York, 1953, Chap. 5.
21. T. A. Ewen, J. Am. Chem. Soc., 106, 6355 (1984).
22. T. Keij, Tokyo: Kadansha, (1972).
23. A. D. Coleman, T. G. Fox, J. Chem. Phys., 38, 1065, (1963).
24. T. Saegusa, H. Imai, J. Furukawa, Makromol. Chem., 64, 224, (1963).
25. T. M. Madkour, J. E. Mark, Macromolecules, 28, 6865, (1995).
26. W. J. Gauthier, J. F. Corrigan, N. J. Taylor, S. Collins, Macromolecules, 28, 3779, (1995).
27. A. Zambelli, P. Locatelli, A. Provasoli, D. R. Ferro, Macromolecules, 13, 267, (1980).
28. G. W. Coates, A.-L. Mogstad, E. Haüptman, M. D. Bruce, R. M. Waymouth, Polym. Prep., 36, 545, (1995).
29. F. A. Bovey, High resolution NMR of macromolecules, Academic Press, New York, 1972.
30. H. N. Cheng, Macromol. Chem. Phys., Theory Simul., 2, 561, (1993).
31. H. N. Cheng, Macromol. Chem. Phys., Theory Simul., 3, 979, (1994).
32. J. Herwig, W. Kaminsky, Polym. Bull. (Berlin), 9, 464, (1983).
33. G. H. Llinas, R. O. Day, M. D. Rausch, J. C. W. Chien, Organometallics, 12, 1283 (1993).
34. H. Brintzinger, D. Fischer, R. Mülhaupt, B. Rieger, R. Waymouth, Angew. Chem. Int., Ed. Engl., 34, 1143, (1995).
35. A. D. Coleman, T. G. Fox, J. Am. Chem. Soc., 85, 1241, (1963).
36. G. G. Odian, Principles of polymerisation, John Wiley & Sons, New York, 1981.
37. T. M. Madkour, A. Soldera, Eur. Polymer. J., 37, 1105, (2001).
38. W. Stocker, S. N. Magonov, H.-J. Cantow, J. C. Wittmann, B. Lotz, Macromolecules, 26, 5915, (1993).
39. T. M. Madkour, J. E. Mark, Comput. Polym. Sci., 4, 79, (1994).
40. T. M. Madkour, J. Chem. Phys., 104, 9154, (1996).
41. T. M. Madkour, J. E. Mark, Polymer, 39, 6085, (1998).
42. T. M. Madkour, J. E. Mark, Polym. International, 44, 331, (1997).
43. L. R. G. Treloar, The physics of rubber elasticity, Oxford University Press, Clarendon, 1975.
44. J. E. Mark, B. Erman, Rubberlike elasticity. A Molecular Primer, Wiley-Interscience, New York, 1988.
45. P. J. Flory, Statistical Mechanics of Chain Molecules, Wiley, New York, 1969.
46. T. M. Madkour, O. M. Ibrahim, A. H. Ebaid, Comput. Polym. Sci., 10, 15, (2000).
47. T. M. Madkour, O. M. Ibrahim, A. H. Ebaid, J. Macromol. Sci., Phys., 39, 679, (2000).
48. J. E. Mark, J. Chem. Phys., 57, 2541, (1972).
49. T. M. Madkour, S. Mohamed, A. M. Barakat, Polymer, 43, 533, (2002).
50. B. Crist, M. J. Hill, J. Polym. Sci., Polym. Phys. Ed., 35, 2329, (1997).
51. L. Mandelkern, in Physical Properties of Polymers, second edition, J. E. Mark, ed., American Chemical Society, Washington, DC, 1993.
52. N. Neuburger, I. Bahar, W. L. Mattice, Macromolecules, 25, 2447, (1992).
53. T. M. Madkour, Chem. Phys., 274, 187, (2001).
54. T. M. Madkour, Angew. Makromol. Chem., 266, 63, (1999).

❑ **Received 14.01.2003, Revieved 05.05.2003**